Talanta 92 (2012) 45–52

Contents lists available at SciVerse ScienceDirect

Talanta

journal homepage: www.elsevier.com/locate/talanta

The solvatochromic effects of side chain substitution on the binding interaction of novel tricarbocyanine dyes with human serum albumin

Garfield Beckford, Eric Owens, Maged Henary, Gabor Patonay*

Department of Chemistry, University Plaza, Georgia State University, Atlanta, GA 30303, USA

ARTICLE INFO

Article history:
Received 11 January 2012
Accepted 13 January 2012
Available online 25 January 2012

Keywords:
Human Serum Albumin (HSA)
Steric specificity
Solvatochromism
Near-infrared laser induced fluorescence (NIR-LIF) spectroscopy
J-aggregation (Bathochromic) and H-aggregation (Hypsochromic)

ABSTRACT

The effects of solvatochromism on protein-ligand interactions have been studied by absorbance and near-infrared laser induced fluorescence (NIR-LIF) spectroscopy. The utility of three novel classes of cyanine dyes designed for this purpose illustrates that the affinity interactions of ligands at the hydrophobic binding pockets of Human Serum Albumin (HSA) are not only dependent on the overall hydrophobic characteristics of the molecules but are highly influenced by the size of the ligands as well. Whereas changes to the chromophore moiety exhibited slight to moderate changes to the hydrophobic nature of these molecules, substitution at the alkyl indolium side chain has enabled us to vary the binding affinity towards serum albumin. Substitution at the indolium side chain among an ethyl to butyl group results in improved binding characteristics and an almost three-fold increase in affinity constant. In addition, replacement of the ethyl side chain with a phenylpropyl group also yielded unique solvotachromic patterns such as increased hydrophobicity and subsequent biocompatibility with the HSA binding regions. Ligand interaction was however inhibited by steric hindrance associated with the bulky phenyl ring system thus affecting the increased binding that could be realized from the improved hydrophobic nature of the molecules. This characteristic change in binding affinity is of potential interest to developing a methodology which reveals information on the hydrophobic character and steric specificity of the binding cavities.

1. Introduction

Recent improvements in near-infrared laser diode technology have attracted considerable interest in the use of near infrared (NIR) cyanine dyes as an analytical tool in bioanalyses and microenvironmental studies [1]. The application of NIR cyanine dyes demonstrates a plethora of photophysical properties making them unique for these areas. Unlike the UV–visible chromophores, only a few molecules exhibit intrinsic autofluorescence in the NIR region of the spectrum (670–1100 nm), [2–7] which provides the advantage of reduced interference from background fluorescence signals [4,8,9]. In addition, NIR assays are of potentially higher sensitivity because of reduced background noise due to Raman or Raleigh Scattering which is $1/\lambda^4$ dependence on the wavelength of the radiation source [5,10,11]. Furthermore, the utility of NIR dyes demonstrates unique hydrophobic characteristics in aqueous solutions that has been quite useful for protein labeling, [3,12] target-specific pH probing, [13–19] drug displacement analysis, [20] DNA sequencing, [12,21,22], and DNA intercalation bioanalytical assays [23,24].

It is well known that NIR cyanine dyes self-aggregate in aqueous buffer solutions resulting from the planar π-electron conjugation systems [4]. It has been reported that the aggregation gives rise to two different structures depending on the angle of slippage (α); these are commonly referred to as J-aggregation (bathochromic) and H-aggregation (hypsochromic) [4,25]. Studies have shown that a small angle of molecular slippage ($\alpha > \sim 32^\circ$) results in H-aggregation while large slippage ($\alpha < \sim 32^\circ$) leads to J-aggregation formation (need more than one r [26,27]. The type of aggregation is largely dependent on the solvent polarity, but it may also be affected by other factors such as temperature, pH, dye concentration and ionic strength [4,27,28]. Kim and coworkers among others have studied the hydrophobic characteristics of the bis(heptamethine cyanine) dyes, but relatively few recent experimental studies have dealt with the trimethine family of dyes [4,11]. Some interesting results have been reported on their hydrophobic behavior and aggregation formation. Such as a prominent red-shifted spectral transition influenced by the increased $\pi \rightarrow \pi^*$ energy gap associated with reduced solvent polarity [11]. As a part of this work, three classes of novel trimethine dyes were prepared to examine the photophysical behavior and the effects of solvatochroism on their binding characteristics. Among these dyes are Benz[*c,d*]indolium, Benz[*e*]indolium and Fischer indolium derivatives with variations made to the symmetrical indolium side chains

* Corresponding author. Tel.: +1 404 413 5556; fax: +1 404 413 5556.
E-mail address: gpatonay@gsu.edu (G. Patonay).

0039-9140/$ – see front matter © 2012 Elsevier B.V. All rights reserved.
doi:10.1016/j.talanta.2012.01.029

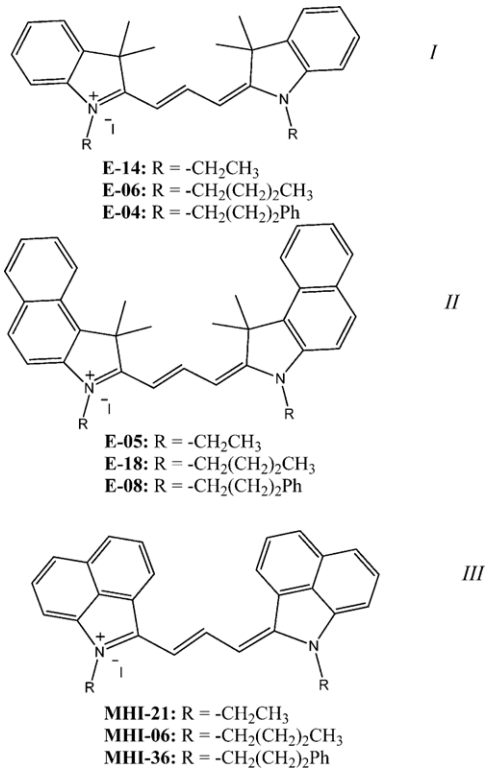

Fig. 1. Molecular structure of Indolium cyanine dyes studied, I; Fischer indole, II; benz[e]indole, and III; benz[c,d]indole structures.

(Fig. 1[I–III]). As expected, the photophysical chemistry of cyanine dyes is determined primarily by the conjugated backbone carbon structure. However, the nature of the polymethine indolium side chains, critical to the overall hydrophobic nature of these fluorescence compounds is the basis of their distinct spectral variations. It has been shown that most NIR cyanine H-aggregates in aqueous media usually display virtually no fluorescence activity [4,29–32]. Interaction with HSA, however, results in a marked increase in fluorescence intensity thus providing a viable option for non-covalent labeling of proteins as well as their utilization as binding site probes.

A full understanding of the binding equilibria can explain the enhanced sensitivity and reduced detection limits attained with NIR dyes for proteomic studies. The spectral characteristics and structure of these probes are determined predominantly by their microenvironment, and any conjugation with biomolecules would subsequently lead to a concomitant change in these intrinsic properties. Furthermore, the polarity of the microenvironment can further influence the spectral properties of these molecules. For example, newly designed cationic dyes are used in investigating the ground and excited states of 1,1′,3,3′-tetraethyl-5,5′,6,6′-tetrachlorobenzimidazolocarbocyanine (TTBC) dyes in solvent [33]. Increased interest in the study of these fluorescence probes has focused tremendously on investigating the non-covalent interaction with proteins for both clinical and biomedical applications [34]. In addition, although more commonly recognized as bio-analytical probes, trimethine cyanine dyes have also demonstrated their suitability as ion selective metal probes for *in vitro* metal ion analyses [35,36].

Non-covalent labeling offers considerable advantages to the numerous applications of cyanine dyes. Studies have reported significant spectral changes with direct interaction of these dyes with the hydrophobic binding pockets of HSA [4,8,9,11,26,37]. Given the importance of serum albumin in maintaining many vital processes, a myriad of new fluorescence probes are being developed to study the hydrophobic effect on binding site specific interactions [38]. Furthermore, NIR fluorescence probes exhibiting spectral profiles that are significantly influenced by solvation are becoming more popular in proteomic studies [3]. Binding of the novel cyanine dyes reported herein with specific protein molecules can provide useful information on binding site location and conformational changes within the target molecules.

Herein, we report a systematic study of the effect of side chain on the spectral properties of three classes of cyanine dyes (Fig. 1). Our studies demonstrate how the nature of the side chain may influence the overall quantum efficiency and other key spectral characteristics of the probes. In addition, the hydrophobicity and molecular size of the indolium side chain have important ramifications for the interaction of cyanine dyes with serum albumin and their bioanalytical applications.

2. Experimental

2.1. Instrumentation

Laser Induced Fluorescence (LIF) emission spectra were acquired using a K2 Spectrofluorometer (ISS, Champaign, IL) equipped with a R298 Hamamatsu Photomultiplier Tube (Bridgewater, NJ). Excitation was achieved with GaAlAs laser diodes (Laser Max, Rochester, NY) at 690 nm. Slit widths were set to 2 mm and integration time of 3 s. Absorption measurements were achieved with a Perkin-Elmer Lambda UV/VIS/NIR (Lambda 50) Spectrophotometer (Norwalk, CT). All measurements were performed in 1 cm quartz cuvettes (VWR, Suwanee, GA, USA).

2.2. Stock Solutions

Stock solutions of the trimethine cyanine dyes were prepared by dissolving the appropriate mass of each compound in methanol to a final concentration of 1.0 mM. All stock solutions were stored in the dark at 4 °C when not in use. Working solutions were subsequently prepared just prior to use by the dilution of the stock to final concentrations with phosphate buffer. Phosphate buffer (10 mM) was prepared from sodium phosphate monobasic (monohydrate) and sodium phosphate dibasic (monohydrate) obtained from Fisher Scientific (Fair Lawn, NJ) to a final pH of 7.2. The water used was nanopure (Bernard Model D4751 ultrapure water system). HPLC grade methanol was obtained from the Aldrich Chemical Company (Milwaukee, WI). Fatty acid free Human Serum Albumin (≥98% purity) was obtained from Sigma–Aldrich (St. Louis, MO). Stock solutions of HSA were prepared from the solid every 24 h by dilution with phosphate buffer and then stored at 16 °C when not in use.

2.3. Hydrophobicity studies

The hydrophobic characteristics of the cyanine dyes were evaluated by acquiring absorbance and emission spectra of the dyes in varying ratios of methanol-nanopure grade water mixture (in the range of 0–100% methanol/water) until there was no further discernable spectral changes, at which point the spectra overlapped as percent methanol increased.

2.4. HSA binding interaction

The HSA binding studies were conducted by titration of a fixed volume of dye at constant concentration (10 μM for absorbance and 1.0 μM for emission) with HSA. Each sample was vortexed for 30 s and then left for 5 min to equilibrate. Analyses were performed until there were no further spectral changes with further addition

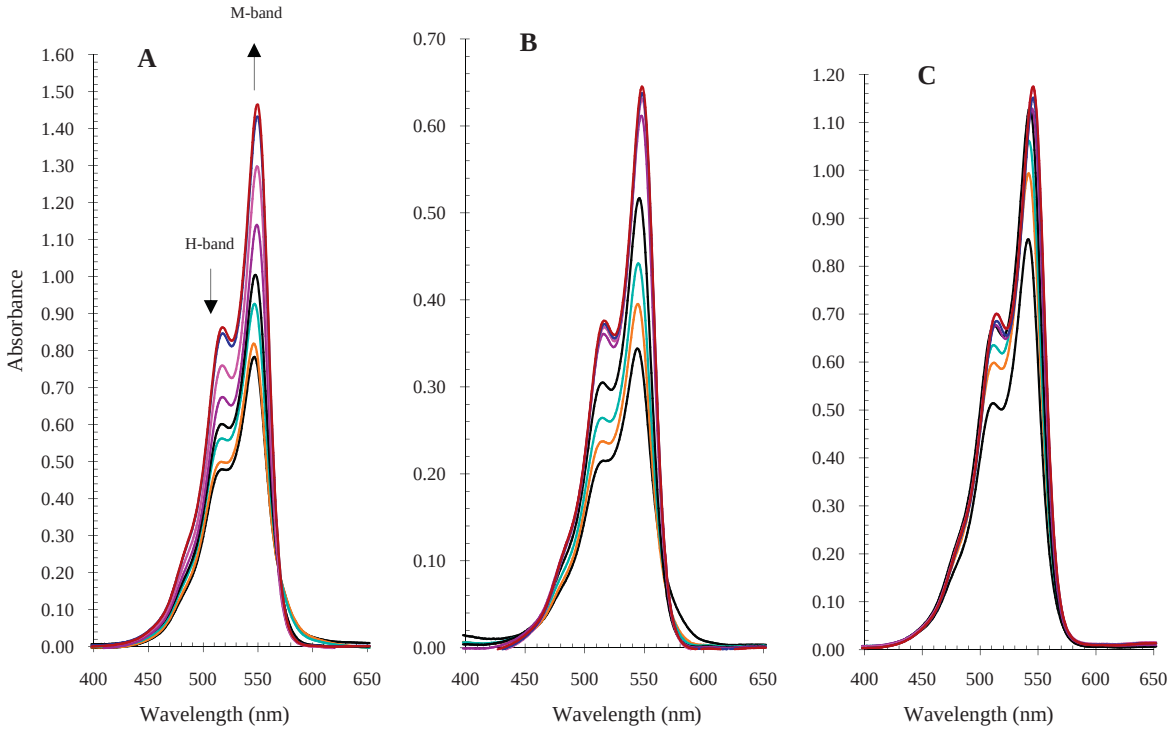

Fig. 2. (A–C) Absorbance of Fischer indolium cyanine dyes as a function of solvent hydrophobicity (%, v/v methanol to buffer) at constant dye concentration of 10 μM. (A) E-04, (B) E-06, (C) E-14. There is a concomitant increase in peak height ratio of monomeric to aggregate peak with increase in methanol to buffer ratio up to 100% methanol.

of the HSA. A fresh batch of the biomolecule solution was prepared every 24 h period.

2.5. Dye synthesis

Symmetrical tricarbocyanine dyes were synthesized by linking two similar nitrogen-containing heterocycles by a three-carbon methine bridge. The common synthetic pathway involved quaternization of the nitrogen atom and base-catalyzed condensation of two salts using triethyl orthoformate. Detailed chemical synthesis of these dyes will be described elsewhere (Henary et al., in preparation). These compounds are designed to display unique photophysical characteristics that directly relate to the heterocyclic structure and *N*-substituted moieties. We described the analyses of three classes of symmetrical tricarbocyanines containing the benz[*c,d*]indole, benz[*e*]indole, and Fischer indole structures. These tricarbocyanines possessed substituents displaying a varied degree of hydrophobicity to study their effects at the hydrophobic binding pockets of HSA.

3. Results and discussion

Solvatochromic effects on the Stokes shift and molar absorptivity of the cyanine dyes

Studies were performed to evaluate the hydrophobic characteristics of three classes of cyanine dyes. As was reported in previous work by Kim et al., NIR molecules typically display moderate to high hydrophobic behavior based on the specific conjugated chromophore as well as the alkyl substituted indolium moiety. There is a general absorbance enhancement of the monomeric band with decreased polarity of the solvent among all three classes of dyes as depicted in Figs. 2–4. Varying the volume ratio of increased methanol to phosphate buffer at constant pH of 7.2 resulted in an increase hydrophobicity of the overall solvent. This change in solvent polarity resulted in characteristic changes in the intrinsic spectral properties of the dyes. As the percent methanol in the solvent increases from 1 to 100% there is a general increase in the ratio of the maximum absorbance intensity of the monomer dye (monomeric or M-band) to the aggregate (Hypsochromic or H-band) absorbance. This increased in absorbance is associate with the breakup of the H-aggregate to form monomers which is evidenced by an increase in the ratio of monomer to aggregate peaks [4]. The aggregation is predominantly due to the plane-to-plane stacking of the dye molecules to form a sandwich type arrangement which is characterized by a broad H-band. Upon exposure to more hydrophobic solvent, this highly organized plane-to-plane arrangement is disrupted which subsequently gives rise to the formation of the randomized monomer arrangement characterized by a sharp M-band. This is further evident in Tables 1A, 1B and 1C whereby the dyes exhibit an increase in the measured molar absorptivity values in less polar solvents such as methanol as opposed to the less hydrophobic buffer solution. Since cyanine dyes are known to exhibit intrinsic H-aggregation in polar solvents, these unique spectral properties make these dyes more attractive as NIR biological probes.

In recent studies Lee et al. reported on the creation of more structurally diverse NIR cyanine dyes by varying the heterocyclic and polymethine fluorophore groups. In fact, they demonstrated that substituting the benz[*c,d*]indolium for a benz[*e*]indolium or a Fischer indolium chromophore resulted in a concomitant blue shift *ca.* 120 nm to the visible region [39]. However this approach creates NIR probes that are less suitable for *in vivo* studies due to the increased light scattering properties associated with the lower band of the spectrum although they may be quite applicable *in vitro*.

In agreement with recently published data by Zhang et al. [26], the increase in chain length and subsequent hydrophobicity of the indolium side chain from the ethyl to butyl moiety among the class **III** type dyes resulted in a blue shift of the absorbance maxima from 764 nm to 758 nm in methanol. While these solvatochromic shifts may indicate interaction between the solvent and the dye in the ground state, a smaller shift suggests that the distribution of the ground state dye is virtually unaffected by the

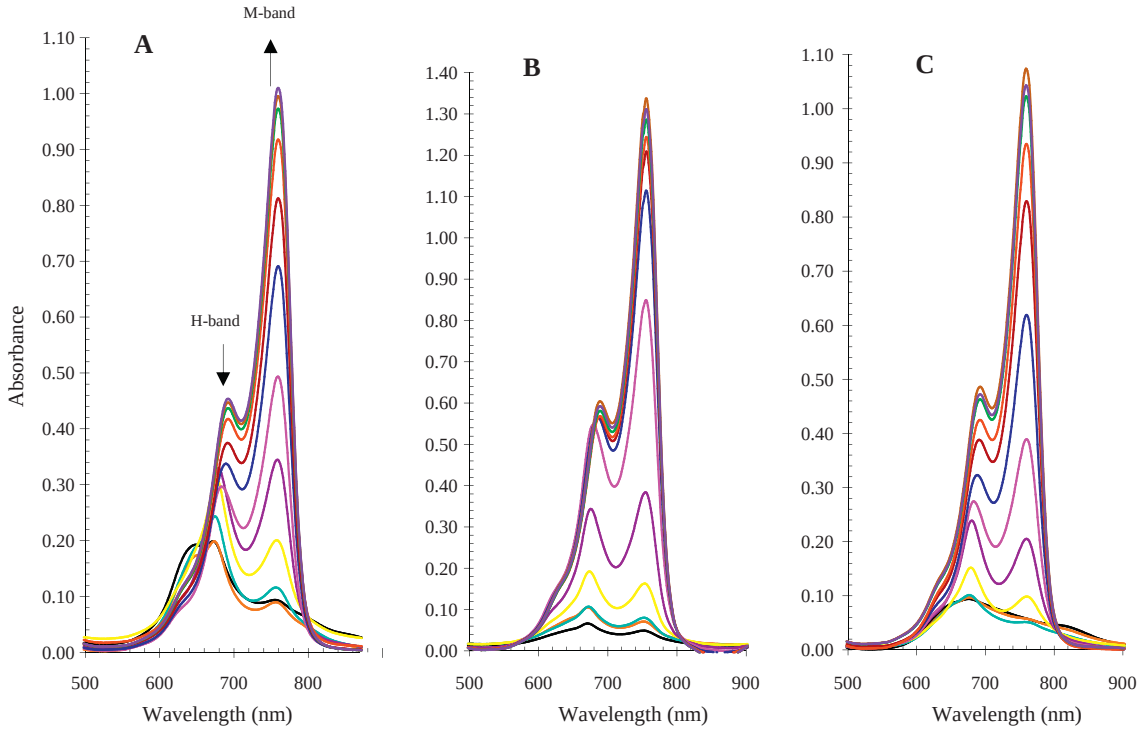

Fig. 3. (A–C) Absorbance of Benz[*c,d*]indolium cyanine dyes as a function of solvent hydrophobicity (%, v/v methanol to buffer) at constant dye concentration of 10 μM. (A) MHI-06, (B) MHI-021, (C) MHI-36. There is a concomitant increase in peak height ratio of monomeric to aggregate peak with increase in methanol to buffer ratio up to 100% methanol.

solvent polarity [40–43]. Unexpectedly, the molar absorptivity was also reduced from143,000 $M^{-1}cm^{-1}$ to 116,000 $M^{-1}cm^{-1}$ due to increased dimerization. From the results, we observed that cyanine dyes bearing less hydrophobic side chains display greater tendencies to self-associate in less polar solvent to form the intramolecular aggregate species. These aggregate species are generally weakly fluorescent and often exhibit a lower molar coefficient than their monomeric counterparts. Similar patterns were observed with the other two classes of NIR molecules. Although effective use of these fluorescent molecules as biological sensors depends significantly on their molecular structure, hydrophobic character is an important factor in their overall biological utility [44]. The incorporation

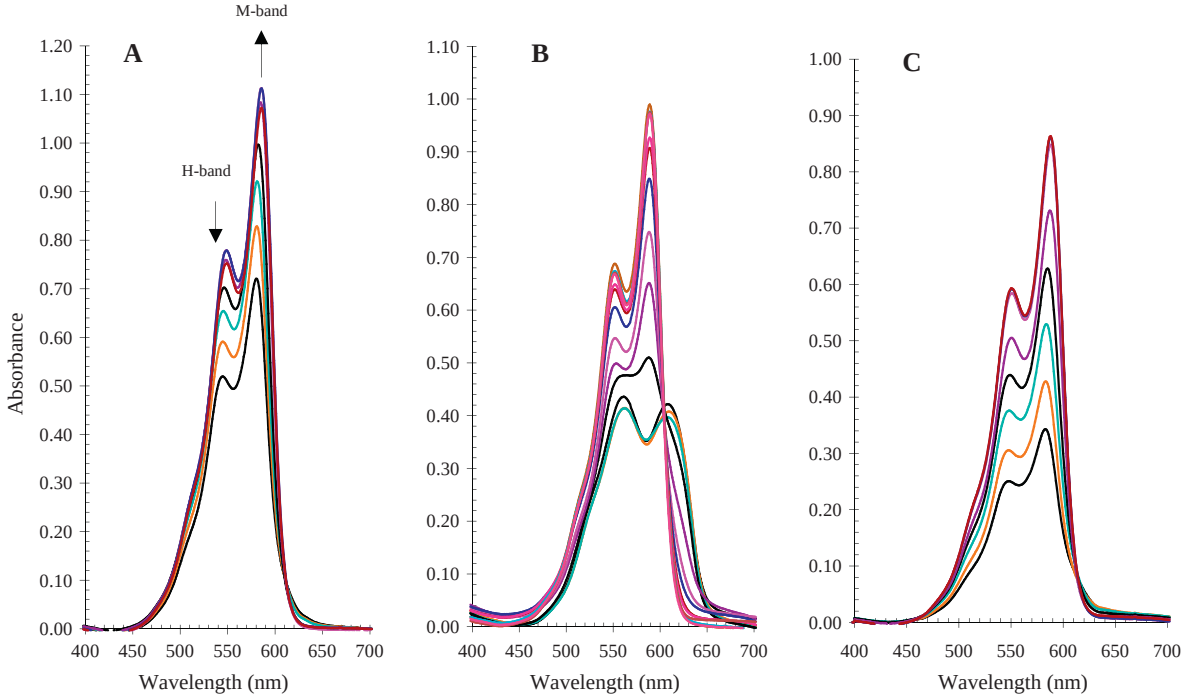

Fig. 4. (A–C) Absorbance of Benz[*e*]indolium cyanine dyes as a function of solvent hydrophobicity (%, v/v methanol to buffer) at constant dye concentration of 10 μM. (A) E-05, (B) E-08, (C) E-18. There is a concomitant increase in peak height ratio of monomeric to aggregate peak with increase in methanol to buffer ratio up to 100% methanol.

Table 1A
Solvent effects on the spectral characteristics of Benz[*c,d*]indolium dyes; MHI-06, 21 and 36.

Solvent	Dyes (λ_{max} [nm]/Em_{max} [nm])			Stokes shift [nm]			Monomeric peak extinction coefficient (ε) mol^{-1} cm^{-1}		
	MHI-06	MHI-21	MHI-36	MHI-06	MHI-21	MHI-36	MHI-06	MHI-21	MHI-36
Water	753/770	755/768	755/773	17	13	18	14,800	16,000	14,500
Methanol	758/774	764/780	758/775	16	16	17	116,000	143,000	124,000
Ethanol	763/778	760/775	760/778	15	15	18	92,400	124,000	108,500
1-Propanol	765/780	763/780	766/780	15	17	14	96,300	127,200	109,400
Sec-butanol	766/780	764/777	766/780	14	13	14	93,100	121,200	101,200
Benzanol	777/797	774/794	777/796	20	20	19	86,600	116,400	104,000
Acetonitrile	757/776	754/772	757/776	19	18	19	95,000	118,500	99,200
DMSO	769/787	771/795	773/798	18	24	25	90,700	116,900	99,200

Table 1B
Solvent effects on the spectral characteristics of Benz[*e*]indolium dyes; E-04, 06 and 14.

Solvent	Dyes (λ_{max} [nm]/Em_{max} [nm])			Stokes shift [nm]			Monomeric peak extinction coefficient (ε) mol^{-1} cm^{-1}		
	E-14	E-06	E-04	E-14	E-06	E-04	E-14	E-06	E-04
Water	541/556	544/559	546/563	15	15	17	96,500	72,000	79,100
Methanol	546/561	548/561	549/565	15	13	16	149,100	106,900	149,500
Ethanol	548/563	550/565	552/567	15	15	15	117,400	92,300	173,400
1-Propanol	550/564	552/566	553/569	14	14	16	115,200	96,500	138,300
Sec-butanol	550/563	552/556	554/568	13	14	14	121,200	102,000	140,900
Benzanol	556/569	559/571	559/575	13	12	16	117,500	98,600	136,500
Acetonitrile	552/559	554/560	555/564	7	6	9	121,000	92,700	147,900
DMSO	552/569	554/569	555/571	17	15	16	110,100	99,800	145,400

Table 1C
Solvent effects on the spectral characteristics of Fischer indolium dyes; E-05, 08 and 18. The solvatochromic effects of side chain substitution on the binding interaction of novel tricarbocyanine dyes with human serum albumin.

Solvent	Dyes (λ_{max} [nm]/Em_{max} [nm])			Stokes shift [nm]			Monomeric peak extinction coefficient (ε) mol^{-1} cm^{-1}		
	E-05	E-08	E-18	E-05	E-08	E-18	E-05	E-08	E-18
Water	580/96	605/617	583/600	16	12	17	62,900	48,000	56,300
Methanol	586/03	589/607	588/605	17	18	17	122,700	117,300	103,300
Ethanol	589/604	592/606	590/605	15	14	15	106,800	77,500	99,100
1-Propanol	590/606	594/608	592/608	16	14	16	109,200	81,700	92,600
Sec-butanol	592/605	595/609	593/607	13	14	14	104,400	81,100	98,200
Benzanol	598/612	601/616	600/614	14	15	14	103,300	83,000	95,900
Acetonitrile	592/601	594/604	586/602	9	10	16	113,200	89,700	99,000
DMSO	592/609	594/610	586/610	17	16	16	104,800	86,300	99,900

of the Benz[*e*]indolium or Fischer indolium chromophore improves quantum efficiency but reduces the hydrophobicity of the molecules. Ideally this improved quantum efficiency results in enhanced optical contrast for *in vivo* studies; however, the diminished hydrophobic nature cannot be overlooked as the molecules have effectively become less biocompatible with regard to their uptake and transportation by key plasma transporter complexes [45]. Despite the potential reduction in the ability to complex biomolecules and subsequent molecular activity resulting from this hydrophobicity change, the effect of the dyes improves solubility is considered quite useful. Moreover, this makes the molecule more attractive as novel NIR biological probes in other aspects such as studying conformational changes in various target proteins [3]. In addition, Figs. 2–4 illustrate that the increased quantum yield associated with the presence of the Benz[*e*]indolium moiety confirms the idea that increased rigidity or reduced free rotation within the molecule is important in reducing photo-isomerization and subsequently stabilizes the ground state distribution of the dyes [46].

Having a comparatively higher Logarithmic Partition (*Log P*) coefficient value of 11.03, **MHI-36** is expected to display more aggregation tendencies than the N-butyl analog in the polar phosphate buffer solution. The *Log P* values are used to determine the distribution ratio of concentrations of the dyes in the two immiscible solvents at equilibrium. Dyes exhibiting higher values are usually more hydrophobic and are thus more suitable for non-polar solvents. However, mere analysis of these data shows, **MHI-36** displayed less favorable aggregation tendencies than **MHI-06** with a *Log P* value of 9.26. This is further illustrated in Table 1A which shows values of 124,000 and 116,000 $M^{-1}cm^{-1}$, respectively. Similar patterns were observed among the classes **I** and **II** type dyes as well. Even though the phenylpropyl derivatives of all three classes of dyes are considerably more hydrophobic with higher *Log P* values, the data did not reveal any significant changes in the overall molar absorptivity values. Thus, it is inferred that the excitation properties of these molecules are not merely governed by hydrophobicity properties but may be further influenced by the molecular conformation of the molecules in different solvent media. However, this pattern was less evident among the individual classes of dyes, whereby the phenylpropyl derivatives continued to display the highest molar absorptivity values which can be further explained by enhanced π–π electron stacking of the indolium aromatic system, an arrangement uncharacteristic of the aliphatic indolium side chains.

3.1. HSA binding interactions with NIR cyanine dyes

The conjugate formation of the cyanine dyes with the serum albumin was studied in phosphate buffer at pH 7.2. The binding interaction was monitored by evaluating the changes in absorbance and emission intensities at a fixed concentration of dye with micromolar concentrations of protein. Based on the dye structure, this

Table 2
Binding affinities of cyanine dyes. Increased hydrophobicity of the indolium side chain resulted in enhanced binding interaction. There is a general increase binding affinity with increased hydrophobicity of the dye. However, beyond a certain ligand size, the increased binding associated with hydrophobicity is limited by steric hindrance of the ligand within the hydrophobic binding cavities.

Cyanine Dye	Indolium side chain	Abs (λ_{max}) [nm]	Em (Em_{max}) [nm]	Molar absorptivity (ε) $M^{-1}cm^{-1}$	*Log P* value[a]	Binding affinities (K_a) $\times 10^5 M^{-1}$	Quantum yield (in methanol)
MHI-06	$-(CH_2)_3CH_3$	758	774	116,000	9.26	10.60	0.0047
MHI-21	$-CH_2CH_3$	764	771	143,000	7.46	1.55	0.0036
MHI-36	$-(CH_2)_3C_6H_5$	758	775	124,000	11.03	3.51	0.0061
E-6	$-(CH_2)_3CH_3$	531	605	106,900	8.57	8.75	0.0112
E-14	$-CH_2CH_3$	529	561	149,500	7.68	7.54	0.0200
E-04	$-(CH_2)_3C_6H_5$	532	565	149,100	10.34	8.03	0.0058
E-18	$-(CH_2)_3CH_3$	572	605	103,000	10.09	8.33	0.0124
E-05	$-CH_2CH_3$	569	603	122,700	9.19	3.25	0.0041
E-08	$-(CH_2)_3C_6H_5$	572	607	117,300	11.60	4.14	0.0171

Indocyanine Green (ICG) is used as standard for quantum yield determination of Benz[*c,d*]indolium dyes, with Φ_f value of 4.2% determined by Reindl et al. [52].
Fluorescein is used as standard for quantum yield determination Benz[*e*]indolium and indolium dyes, with Φ_f value of 79% determined by Magde et al. [53].
[a] PC MODEL v. 9.0.

results in up to as much as a five-fold increase in absorbance intensity of the monomeric peak among all three families of dyes.

Previous research by Kim et al. suggested that most cyanine dyes bind in a 1:1 stoichiometry with HSA, [11,26,38,47]. This arrangement is confirmed by the Job's Plot method [48]. A method of continuous variation of both dye and HSA concentrations (varied dye to HSA ratio) at constant total concentration yielded maximum absorbance intensity at 0.492 HSA mole fraction, which, by application of the Job's method, corresponds to a 1:1 binding stoichiometry. Assuming all the NIR probes are conjugated with the free HSA, an equilibrium is reached. In order to determine the binding affinities of the NIR cyanine, the binding interactions were evaluated with the Scatchard method [4,8,26,35,36]. In accordance with this method, the concentrations (activities) of the different

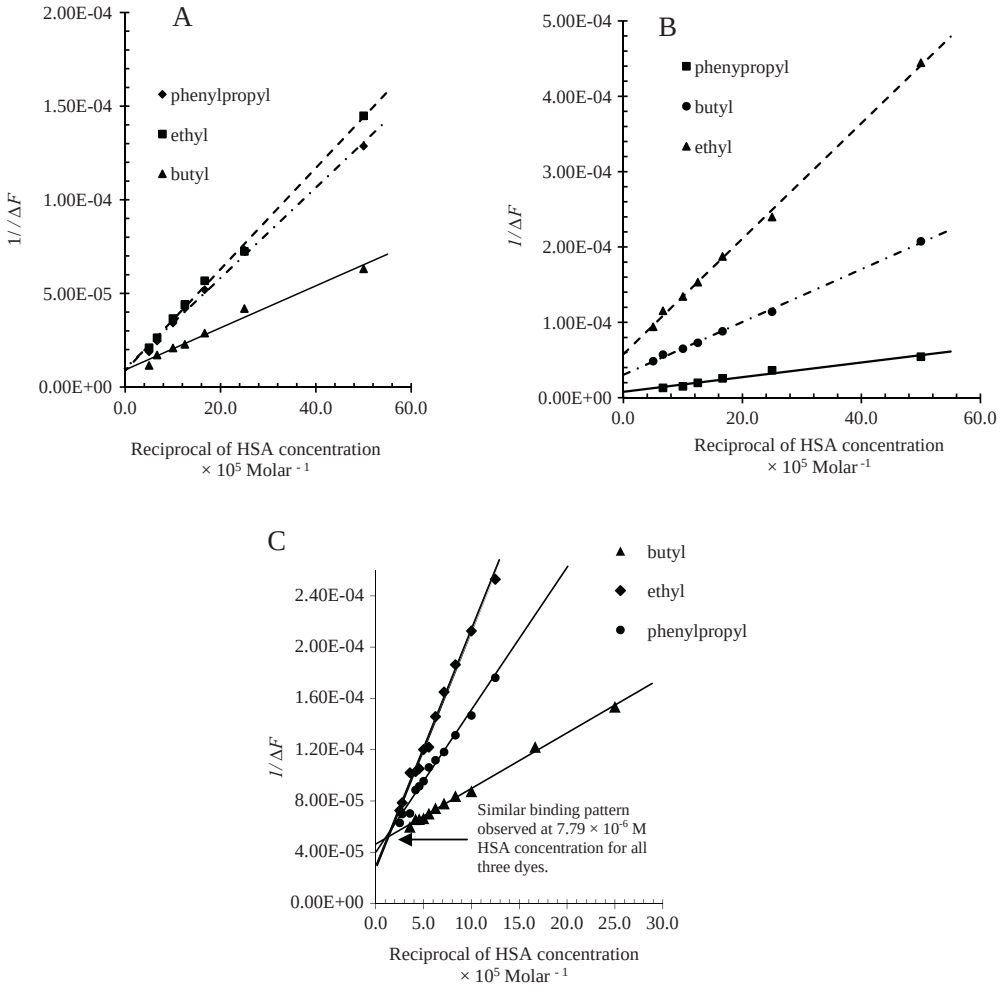

Fig. 5. (A–C) Scatchard Plots of cyanine dyes at constant concentration of 1.0 μM and increasing HSA concentration in the 0–2.0 μM range. Graph (A) Benz[*e*]indolium cyanine, (B) Fischer Indolium cyanine, and (C) Benz[*c,d*]indolium cyanine dyes with different indolium substituents.

reaction species are measured at equilibrium. Applying the equation, K_s

$$\text{Dye} + \text{HSA} \overset{K_s}{\rightleftharpoons} \text{Dye} - \text{HSA} \quad (1)$$

and assuming activity coefficient to be unity (and 1:1 reaction stoiciometry), K_s

$$K_s = \frac{[\text{Dye} - \text{HSA}]}{[\text{Dye}]\,[\text{HSA}]} \quad (2)$$

the affinity constant is determined from the linear fit of the data of the fluorimetric titration of a fixed concentration of dye with HSA according to Eq. (3) [4,8,26,35,36].

$$\frac{1}{\Delta F} = \frac{1}{k[\text{Dye}]} + \left(\frac{1}{k[\text{Dye}]K_s}\right)\frac{1}{[\text{HSA}]} \quad (3)$$

where ΔF is the change in emission intensity of the Dye–HSA conjugate and k is a constant that is dependent on the quantum efficiency of the process and the instrumentation. A plot of the reciprocal of ΔF *versus* the reciprocal of HSA concentration should give a linear relationship that intersects the ordinate (*x-axis*) as depicted in Fig. 3A–C. The affinity constant is calculated by dividing the intercept by the slope of the line.

Having displayed moderate affinities for the serum albumin, the variation in the alkyl indolium moiety of the cyanine dyes had a profound effect on overall conjugation with the biomolecule. In recent literature Kim and coworkers characterized the hydrophobic binding pockets of the HSA molecule [11,38] and observed that changes in binding affinity are attributed to the substitution of hydrophobic moieties at the heterocyclic ring of the cyanine dyes. Table 2 summarizes the effects of indolium side chain modifications on the binding affinity of these novel cyanine molecules.

As previously mentioned, cyanine dyes self-assemble in polar solvents such as the phosphate buffer solution owing to the strong intermolecular van der Waals interactions between the heterocyclic moieties to form H-aggregation [4]. Conjugate formation with HSA disrupts the aggregation thereby increasing monomer formation and subsequently increasing fluorescence emission and molar absorptivity values of the bound dye.

It was suggested that cyanine dyes are binding site specific and exhibit a high specificity for the subdomain III commonly referred to as the site II of the HSA molecule [9,49,50]. Within this context these investigations suggested that the binding affinity of these dyes is not only hydrophobicity dependent, but may be influenced by steric interferences within the binding sites. There is a general pattern of increased binding affinity with increased hydrophobicity among the dyes and at pH 7.2 it is unlikely that the delocalized positive charge on these molecules will have any electrostatic effect within the binding cavity. However, further analysis of the data as shown in Table 2 reveals that among the class **III** derivatives, despite **MHI-36** exhibiting a binding constant of $3.51 \times 10^5\ \text{M}^{-1}$, it is the most hydrophobic of the class (as indicated by the hydrophobicity 11.03 *Log P* value). In comparison to the other two analogs, there is increased binding when the more hydrophobic phenylpropyl group is substituted with the less hydrophobic butyl moiety with a *Log P* value of 9.26.

Although it is a general trend for the more hydrophobic group to bind more strongly to the valine rich hydrophobic pocket of the HSA, to the contrary, our conjugation experiments yielded some unexpected binding results. This type of binding pattern resulted from the occurrence of steric hindrances within the binding cavities which increases with the presence of the more bulky indolium side chain aromatic system. Therefore it can be inferred that beyond a certain ligand size steric factors will decrease binding affinity with the HSA molecule. Interestingly, inspite of the variation in binding patterns, extrapolation of the linear Scatchard plot of Fig. 5C illustrates that at HSA of concentration of 7.97×10^{-6} M all three class **III** cyanine dyes yielded similar binding parameters. As depicted in the figure, at this concentration and in the absence of the biomolecule, the unconjugated dye remains in the virtual non-fluorescing aggregated form. It is thus believed that the emission intensity of the bound dye is primarily dependent on the degree of conjugation and is unaffected by the hydrophobicity of the solvent when the biomolecule is added. In addition, recent studies have revealed that the interaction of bulky hodrophobic ligands with HSA can lead to the perturbation of the secondary conformation. This may further result in the rearrangement of I–II and II–III domain interfaces and conformation changes of the key hydrophobic binding sites [51]. Similarly, the Scatchard plots of the class **I** and **II** dyes also illustrate that the binding affinity is dependent on the hydrophobicity but is further influenced by steric size of the indolium side chain of the dyes. However, for the former families of dyes, the binding data did not support the theory of similar binding patterns at a specific HSA concentration. In addition, the more conjugated heterocyclic class **III** derivatives have proven to bind more strongly with the biomolecule as indicated by the comparatively higher binding constants ranging from 3.51 to $10.60 \times 10^5\ \text{M}^{-1}$ despite the influence of steric hindrance.

Albumin is known to bind a large variety of other compounds such as fatty acids, nucleic acids and oligoproteins and antibodies; thus, it is of potential interest to develop methods that can reveal information on the hydrophobic character and steric specificity of the binding cavities. This unique binding effect of these novel NIR cyanine probes further demonstrates the utility of a host of bioanalytical applications including monitoring changes in protein binding sites, conformational changes and activities of biological molecules and target proteins.

4. Conclusions

The utility of near-infrared cyanine dyes in biomedical and clinical research highlights their unique hydrophobic characteristics in aqueous solutions and has been quite useful for protein labeling, DNA sequencing, DNA intercalation, *in vivo* tissue imaging among numerous other bioanalytical assays. Owing to the ability to self-aggregate in polar solvents due to the planar π–π electron conjugation systems, changes in the hydrophobic moieties of the dyes serve a viable option of monitoring binding affinity with biomolecules such as serum albumin. In addition to the enhanced binding site specificity, the unique hydrophobic behavior of the three classes of cyanine dyes presented in this article reveals photophysical properties that are suitable for binding site characterization and changes the overall 3-dimensional structure. Whereas previous results have sought to examine the effect of hydrophobicity on the overall conjugate formation of these fluorescence chromophores with serum albumin, these studies demonstrate how the combination of ligand size and hydrophobic properties may also affect conjugation. There is a general pattern of increased binding affinity with increased hydrophobicity among these dyes. However, this pattern is also affected by steric hindrance beyond a certain ligand size. Nonetheless, further studies are needed to fully examine the utility of the hydrophobic characterization of these novel tricarbocyanine chromophores for binding site specific bioanalytical assay. Besides it would be quite useful to establish a relationship between ligand size and hydrophobic properties for key albumin binding small molecules.

Acknowledgements

We thank Abbott Pharmaceuticals *(formerly Solvay)* for support of this research. Also, thank Sang Hoon Kim and Shirlene Jackson-Beckford for their assistance in setting up the experimental methods.

References

[1] N.L. Martirosyan, D.D. Cavalcanti, J.M. Eschbacher, P.M. Delaney, A.C. Scheck, M.G. Abdelwahab, P. Nakaji, R.F. Spetzler, M.C. Preul, Journal of Neurosurgery 115 (2011) 1131.
[2] T.G.G. Vo-Dinh, in: G. Gauglitz, T. Vo-Dinh (Eds.), Handbook of Spectroscopy, vol. 2, Wiley-VCH, Cambridge, 2003.
[3] M.Y. Berezin, H. Lee, W. Akers, S. Achilefu, Biophysical Journal 93 (2007) 2892.
[4] J.S. Kim, R. Kodagahally, L. Strekowski, G. Patonay, Talanta 67 (2005) 947.
[5] J. Klohs, A. Wunder, K. Licha, Basic Research in Cardiology 103 (2008) 144.
[6] L. Tarazi, A. George, G. Patonay, L. Strekowski, Talanta 46 (1998) 1413.
[7] S.J. Zhuo, H. Zheng, J.L. Chen, D.H. Li, Y.Q. Wu, C.Q. Zhu, Talanta 64 (2004) 528.
[8] F. Welder, B. Paul, H. Nakazumi, S. Yagi, C.L. Colyer, Journal of Chromatography B: Analytical Technologies in the Biomedical and Life Sciences 793 (2003) 93.
[9] J. Sowell, K.A. Agnew-Heard, J.C. Mason, C. Mama, L. Strekowski, G. Patonay, Journal of Chromatography B 755 (2001) 91.
[10] M. Lowry, S.O. Fakayode, M.L. Geng, G.A. Baker, L. Wang, M.E. McCarroll, G. Patonay, I.M. Warner, Analytical Chemistry 80 (2008) 4551.
[11] G. Patonay, J.S. Kim, R. Kodagahally, L. Strekowski, Applied Spectroscopy 59 (2005) 682.
[12] T. Biver, A. Boggioni, F. Secco, E. Turriani, M. Venturini, S. Yarnaoluk, Archives of Biochemistry and Biophysics 465 (2007) 90.
[13] M. Puyol, C. Encinas, L. Rivera, S. Mijtsov, J. Alonso, Dyes and Pigments 73 (2007) 383.
[14] M. Puyol, C. Encinas, L. Rivera, S. Miltsov, J. Alonso, Sensors and Actuators B: Chemical 122 (2007) 53.
[15] Y.F. Xu, Y. Liu, X.H. Qian, Journal of Photochemistry and Photobiology A: Chemistry 190 (2007) 1.
[16] Z.R. Zhang, S. Achilefu, Chemical Communications (2005) 5887.
[17] A.E. Boyer, M. Lipowska, J.M. Zen, G. Patonay, V.C.W. Tsang, Analytical Letters 25 (1992) 415.
[18] R.J. Williams, M. Lipowska, G. Patonay, L. Strekowski, Analytical Chemistry 65 (1993) 601.
[19] M.D. Antoine, S. Devanathan, G. Patonay, Microchemical Journal 45 (1992) 36.
[20] C. Andre, Y. Jacquot, T.T. Truong, M. Thomassin, J.F. Robert, Y.C. Guillaume, Journal of Chromatography B: Analytical Technologies in the Biomedical and Life Sciences 796 (2003) 267.
[21] Y.Y. Davidson, B.M. Gunn, S.A. Soper, Applied Spectroscopy 50 (1996) 211.
[22] T.P. Constantin, G.L. Silva, K.L. Robertson, T.P. Hamilton, K. Fague, A.S. Waggoner, B.A. Armitage, Organic Letters 10 (2008) 1561.
[23] V. Karunakaran, J.L.F. Lustres, L.J. Zhao, N.P. Ernsting, O. Seitz, Journal of the American Chemical Society 128 (2006) 2954.
[24] T.L. Netzel, M. Zhao, K. Nafisi, J. Headrick, M.S. Sigman, B.E. Eaton, Journal of the American Chemical Society 117 (1995) 9119.
[25] V. Kumar, G.A. Baker, S. Pandey, Chemical Communications 47 (2011) 4730.
[26] Y.Z. Zhang, H.Y. Du, Y.L. Tang, G.Z. Xu, W.P. Yan, Biophysical Chemistry 128 (2007) 197.
[27] Y.Z. Zhang, J.F. Xiang, Y.L. Tang, G.Z. Xu, W.P. Yan, Dyes and Pigments 76 (2008) 88.
[28] J.K. Jin, J.Z. Sun, Y.Q. Dong, H.P. Xu, W.Z. Yuan, B.Z. Tang, Journal of Luminescence 129 (2009) 19.
[29] W.Y. Yan, C.L. Colyer, Journal of Chromatography A 1135 (2006) 115.
[30] A.S. Kashin, A.S. Tatikolov, High Energy Chemistry 43 (2009) 480.
[31] A.S. Tatikolov, A.A. Ishchenko, M.A. Kudinova, I.G. Panova, High Energy Chemistry 44 (2010) 304.
[32] Y.Z. Zhang, Q.F. Yang, H.Y. Du, Y.L. Tang, G.Z. Xu, W.P. Yan, Chinese Journal of Chemistry 26 (2008) 397.
[33] S. Karaca, N. Elmaci, Computational and Theoretical Chemistry 964 (2011) 160.
[34] F. Luschtinetz, C. Dosche, M.U. Kumke, Bioconjugate Chemistry 20 (2009) 576.
[35] L. Tarazi, H. Choi, J.C. Mason, J. Sowell, L. Strekowski, G. Patonay, Microchemical Journal 72 (2002) 55.
[36] L. Tarazi, N. Narayanan, G. Patonay, Microchemical Journal 64 (2000) 247.
[37] G. Patonay, J. Salon, J. Sowell, L. Strekowski, Molecules 9 (2004) 40.
[38] M.Y. Berezin, H. Lee, W. Akers, G. Nikiforovich, S. Achilefu, Photochemistry and Photobiology 83 (2007) 1371.
[39] H. Lee, M.Y. Berezin, M. Henary, L. Strekowski, S. Achilefu, Journal of Photochemistry and Photobiology a-Chemistry 200 (2008) 438.
[40] M.A. Rauf, J.P. Graham, S.B. Bukallah, M.A.S. Al-Saedi, Spectrochimica Acta Part a-Molecular and Biomolecular Spectroscopy 72 (2009) 133.
[41] F.L. Dickert, U. Geiger, P. Lieberzeit, U. Reutner, Sensors and Actuators B: Chemical 70 (2000) 263.
[42] B. Jedrzejewska, M. Pietrzak, J. Paczkowski, Journal of Fluorescence 20 (2010) 73.
[43] M.J. Sawicka, J.A. Soroka, E.K. Wroblewska, I.K. Zawadzka, Polish Journal of Chemistry 80 (2006) 1337.
[44] S.H. Kim, S.Y. Lee, S.Y. Gwon, Y.A. Son, J.S. Bae, Dyes and Pigments 84 (2010) 169.
[45] X.H. Gao, L.L. Yang, J.A. Petros, F.F. Marshal, J.W. Simons, S.M. Nie, Current Opinion in Biotechnology 16 (2005) 63.
[46] S. Murphy, G.B. Schuster, Journal of Physical Chemistry 99 (1995) 8516.
[47] A.J. Sophianopoulos, J. Lipowski, N. Narayanan, G. Patonay, Applied Spectroscopy 51 (1997) 1511.
[48] Y.Y. Zhou, H.W. Xu, H.P. Yu, L. Chun, Q. Lu, L. Wang, Spectrochimica Acta Part A: Molecular and Biomolecular Spectroscopy 70 (2008) 411.
[49] J. Sowell, J.C. Mason, L. Strekowski, G. Patonay, Electrophoresis 22 (2001) 2512.
[50] E. Peyrin, Y.C. Guillaume, C. Guinchard, Biophysical Journal 77 (1999) 1206.
[51] S.-i. Fujiwara, T. Amisaki, Chemical & Pharmaceutical Bulletin 59 (2011) 860.
[52] S. Reindl, A. Penzkofer, S.H. Gong, M. Landthaler, R.M. Szeimies, C. Abels, W. Baumler, Journal of Photochemistry and Photobiology A: Chemistry 105 (1997) 65.
[53] D. Magde, R. Wong, P.G. Seybold, Photochemistry and Photobiology 75 (2002) 327.